HOW DOES THE MAGNETIC CYCLE CHANGE RADIANCE AND IRRADIANCE OF THE SUN?

Sami K. Solanki

Max-Planck-Institut für Aeronomie, 37191 Katlenburg-Lindau, Germany
tel: +49 5556-979-325 / fax: +49 5556-979-190
e-mail:solanki@linmpi.mpg.de

ABSTRACT

The Sun's magnetic field, which is concentrated into flux tubes in the photosphere, affects the radiance. Depending on the size of a flux tube it radiates more (for slender tubes) or less (for broad tubes) strongly than the quiet Sun. The Sum of all magnetic features on the whole solar disc affects the Sun's irradiance. As the number and the size distribution of the flux tubes changes over the solar cycle it produces a variation of total irradiance, which is very similar to the observed variation. There is also evidence that the Sun's magnetic field exhibits a secular variation, which is expected to produce a slow irradiance change, whose amplitude is expected to be larger than the cyclic variation. In this review some of the relevant processes taking place in flux tubes are pointed out and models describing the irradiance variations over the solar cycle based on the Sun's magnetic field are discussed. Finally, the results of the modelling of the secular variation of the Sun's magnetic field are presented.

1. INTRODUCTION

The face of the Sun changes completely between solar activity minimum and maximum. The number of sunspots, the area covered by faculae and plages, the number of bright coronal loops, flares, equatorial coronal holes and CMEs all increase dramatically with increasing magnetic flux. Even the Sun seen as a star exhibits significant variations over the solar cycle. Thus the equivalent width of the He I 10830Å and the frequencies of low-degree p-modes display a cyclic behaviour. Variations are also seen both in total irradiance (see Lean & Fröhlich 2002) and in irradiance at different wavelengths, e.g. in the EUV, or in the cores of strong, chromospheric lines (e.g. Ca II H + K cores, or the Mg II core-to-wing ratio; see Hall 2002; Woods 2002.

Most and possibly even all these variations are caused by the cyclic variation of the Sun's magnetic field. In this paper I consider how the magnetic field and its change over the solar cycle affects solar radiance and irradiance, whereby the irradiance is the integral over all radiances from the solar disc.

2. MAGNETIC FLUX TUBES AND SOLAR RADIANCE

The influence of the magnetic field on radiance is often complex and sometimes subtle. It depends on a number of parameters, such as the magnetic flux density (or spatially averaged field strength), the location on the solar disc and the observed wavelength range. Let us consider first the radiance at the centre of the solar disc. The dependence of brightness on magnetogram signal (a measure of the line-of-sight flux per pixel, or longitudinal magnetic field strength averaged over the pixel) for 3 different wavelengths is plotted in Figure 1: visible continuum, the core of the photospheric absorption line, Fe I 5250.2Å, and the chromospheric emission core of the Ca II K line (Leighton 1959; Schrijver et al. 1989; Harvey & White 1999). The difference in the dependence of contrast on magnetogram signal, $\langle B\cos\gamma\rangle$, at the 3 wavelengths is clear. Here B is the intrinsic field strength in the magnetic flux tubes found within the resolution element, γ is the angle between the magnetic vector and the line of sight and the brackets denote averaging over the resolution element.

How are these dependences to be understood? Firstly, we need to note that in faculae and the network, i.e. at the magnetogram signals considered in Figure 1, the magnetic field is concentrated into elements of flux, often called flux tubes, all except the largest of which are spatially unresolved. In the photosphere, flux tubes typically have a field strength of 1–1.5 kG. As $\langle B\cos\gamma\rangle$ increases then basically the magnetic filling factor (and average flux tube cross-sectional area) increases. The filling factor denotes the fraction of the solar surface within the spatial resolution that is covered by a kilo-Gauss field (or, equivalently, by magnetic flux tubes). The intrinsic magnetic field strength of the flux tubes does not change significantly with size or filling factor (see Solanki at al. 2000). Thus the initial increase in contrast with $\langle B\cos\gamma\rangle$ does not signify that the individual flux tubes are becoming brighter, but rather that they are becoming more visible, as they fill more of a pixel. Actually the brightness per unit magnetic flux (or the intrinsic contrast of a flux tube) decreases steadily with increasing $\langle B\cos\gamma\rangle$, or increasing cross-sectional area of the flux tube (e.g., Solanki & Brigljević 1992; Keller 1992;

Proc. SOHO 11 Symposium, 'From Solar Min to Max: Half a Solar Cycle with SOHO', Davos, Switzerland, 11-15 March 2002 (ESA SP-508, June 2002)

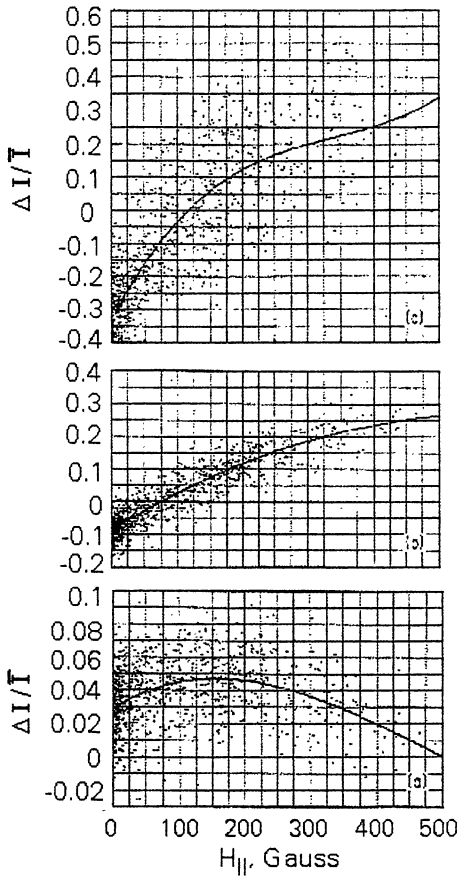

Figure 1. Dependence of the brightness contrast on the magnetogram signal (average longitudinal field strength) at three wavelengths. Bottom: Continuum, middle: core of the photospheric line Fe I 5250.2Å, top: core of the chromospheric line Ca II K. The average photospheric values are where the fit curves interest the ordinates. (from Frazier 1971).

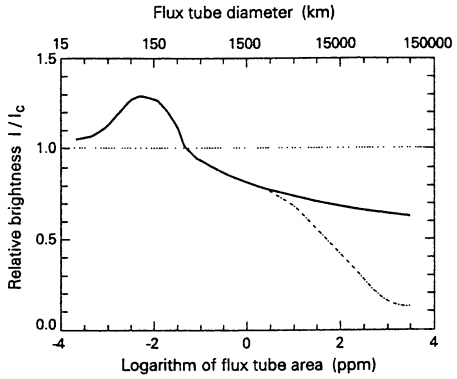

Figure 2. White-light brightness of magnetic features relative to 'quiet' Sun brightness vs. the (logarithmic) area of magnetic features in 10^{-6} times the solar hemispheric area (lower axis) and their diameter (upper axis). The solid line represents the brightness averaged over the whole flux tube, i.e., over both umbra and penumbra for sunspots. The dot-dashed line represents the brightness of the umbra only..

Ortiz et al. 2002). This is illustrated in Figure 2, where the approximate white-light brightness of individual flux tubes relative to the quiet Sun brightness is plotted vs. their size. Whereas the small flux tubes (which dominantly compose faculae and the network) are bright, this is not the case for larger features, the pores and sunspots. For the sunspots two values have been plotted, the contrast of the dark parts of the umbra (lower, dot-dashed curve) and the contrast averaged over the whole sunspot (upper curve). Figure 2 explains why in Figure 1 the continuum contrast saturates and starts to decrease again with increasing $\langle B \cos\gamma \rangle$, eventually turning negative.

From Figure 1 it is obvious, however, that the contrast behaves quite differently in the cores of both photospheric and chromospheric lines than in the continuum. The line cores are formed higher in the solar atmosphere than the continuum, and since the cores of both lines are strongly coupled to the temperature this suggests that a) the spatially averaged temperature contrast in small flux tubes increases rapidly with height, b) for flux tubes of intermediate size the temperature can be lower than in the surroundings in the continuum-forming layers, but higher in the upper photosphere and the chromosphere. For sunspots, which lie outside the range of Figure 1, photospheric line cores show similar negative intensity contrasts as the continuum, while in the chromosphere a slight positive contrast is seen (Sütterlin 1998).

In Figure 3 I plot the temperature stratification of two types of small flux tubes, together with that of the quiet Sun. The brighter of these flux tubes are smaller (100–200 km diameter) and are more common in the quiet Sun network, while the less bright ones are somewhat larger and are more abundant in active region faculae. Note, that the temperature in the two types of flux tubes differs mainly in the low photosphere and becomes increasingly similar higher in the atmosphere. Figure 3 provides only a part of the answer, however, why small, spatially unresolved flux tubes produce larger contrasts in the upper photosphere and chromosphere. Another part has to do with the expansion of the flux tubes with height. The magnetic field in a flux tube is confined by the excess gas pressure in the surrounding photosphere. As the gas pressure decreases with height, so does the confining force and the magnetic field expands accordingly. For a spatially unresolved flux tube this has the same effect as when the filling factor were to increase with height, so that the contrast observed at a given spatial resolution increases as well. These effects play a role not just for spectral line radiation, but also for continuum radiation coming from different heights. Thus, in the UV the contrast increases rapidly towards shorter wavelength (e.g. Foukal et al. 1991), at which the radiation originates from higher layers. The increase in temperature sensitivity of the Planck function towards smaller wavelengths plays only a minor role in determining this wavelength dependence of the contrast.

Looking again at Figure 1 we note that the scatter of the points representing the Ca II K line core contrast is considerably larger than for the other wavelengths. This large

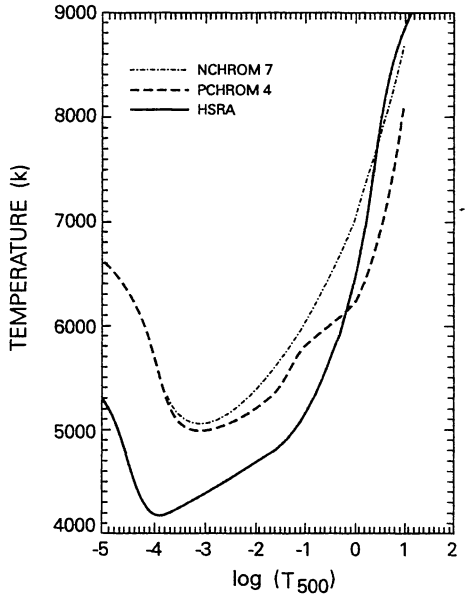

Figure 3. Temperature stratifications as a function of continuum optical depth τ_{500} of the quiet Sun (solid curve) and of two flux tube models, one for network flux tubes (dot-dashed curve), the other for flux tubes in active region plage areas (dashed curve). Figure from Briand & Solanki (1995).

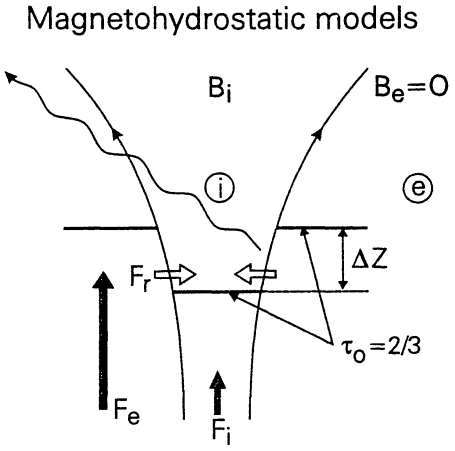

Figure 4. Concept of the magnetohydrostatic flux tube model. One level of constant optical depth in the continuum, $\tau_0 = 2/3$, is shown, with the Wilson depression ΔZ. The hatched arrows F_i and F_e stand for the flux densities in the energy flows inside and outside the flux tubes, respectively. The horizontal arrows indicate the influx of radiation into the transparent top part of the tube. The resulting bright walls are best seen in observations toward the solar limb (as seen along the oblique wavy arrow; figure adapted from Zwaan & Cramer 1989).

scatter is confirmed by later studies (e.g., Skumanich et al. 1975; Schrijver et al. 1989), indicating that there is no simple one-to-one relationship between magnetic field and chromospheric heating, although the presence of a connection is unmistakable. Partly this scatter is caused by the variability of the chromospheric radiation.

The contrast at the different wavelengths illustrated in Figure 1 has different physical causes. The main parameter determining the different behaviour of the contrast and the underlying physical cause is the height of formation of the radiation. In the continuum, and partly also in the cores of photospheric lines, it is due to the heating of the bottom and the walls of the flux tube by radiation. Flux tubes are partly evacuated, so that the optical depth unity level within them lies lower than in the surrounding field-free gas. This effect is well known as the Wilson depression within sunspots, and is present to a lesser extent also in small flux tubes. The geometry of the $\tau = 1$ level and the direction of the radiative flux in a small flux tube is illustrated in Figure 4. In addition to the radiation flowing upwards inside the tube there is now also radiation streaming in from the sides through its walls. Due to the presence of convection, which is by far the most efficient energy transport mechanism just below the solar surface, outside the tube, but not inside it, the walls tend to be hotter than the bottom of the tube for all but the narrowest tubes. This contrast between wall and bottom brightness is small for very slender tubes, but increases rapidly with increasing flux tube size (Knölker & Schüssler 1988). For flux tubes with a width greater than 250-300 km, the bottom of the tube becomes cooler than the $\tau = 1$ level in the normal, field-free photosphere.

Now, when looking at a flux tube along its axis vertically from above we see mainly the bottom and comparatively little of the walls. This is the situation for a vertical flux tube located at the centre of the solar disc. The decrease in contrast for large $\langle B \cos\gamma \rangle$ (Frazier 1971; Foukal & Fowler 1984; Topka et al. 1992, 1997; Ortiz et al. 2002 and others; see Figure 1) is thus best explained by the decreasing brightness of the flux tube bottom with increasing size. This interpretation is supported by other independent analyses and observations (e.g. Keller 1992; Grossmann-Doerth et al. 1994). Nearer to the limb a part of the bottom of the flux tube is hidden by the wall on the Sun-centre side, but the opposite (limb-side) wall becomes better visible. Since the walls are in general brighter than the bottom this leads to an increase of the continuum contrast with decreasing distance to the solar limb (or decreasing $\mu = \cos\theta$, where θ is the heliocentric angle). Finally, for sufficiently small μ, the view of the further or limb-side wall also starts getting blocked, so that the contrast due to the hot wall effect starts to decrease again close to the limb. The angle at which the largest contrast is reached, θ_{max}, is assumed to be the location at which the cooler flux tube bottom is just obscured completely, while leaving a maximum of the hot wall visible. For the special case of a cylindrical tube of radius $R_{\rm ft}$ we have

$$\tan\theta_{max} = 2R_{\rm ft}/\Delta Z,$$

where ΔZ is the Wilson depression (Spruit 1976).

The work of Topka et al. (1997) and Ortiz et al. (2002), who analyze the centre-to-limb variation (CLV) of magnetic features, shows a qualitative agreement with the

predictions of the hot wall model. The very different CLVs displayed by features with different $\langle B \cos\gamma \rangle$ confirms that the flux tubes are larger in regions with larger $\langle B \cos\gamma \rangle$ and that the contrast between the brightness of the bottom and the wall is also enhanced. Interesting is the fact that the network magnetic elements show a relatively flat contrast as a function of μ, quite unlike the active region faculae. It was on the basis of the form of the CLV of the latter that Kuhn et al. (1988) argued that magnetic fields are not the cause of the variation of the Sun's total irradiance over the solar cycle. The main feature entering their argument is that the facular contrast is small (and even negative) at disc centre, but strong and positive near the limb. In view of these new results regarding the flat and positive CLV of the network contrast, the claim of Kuhn et al. (1988) needs to be looked at again carefully (cf. Foukal et al. 1991).

The above only describes the CLV of the continuum contrast. When considering spectral lines which are formed over a larger range of continuum optical depth other effects also start playing an important role. Individual flux tubes become partly optically thin when seen from the side, so that radiation from inside the flux tubes gets mixed with radiation from the surroundings (along a single line of sight). This leads to a much less strong rise of the contrast in spectral line cores towards the limb (e.g., Skumanich et al. 1984). UV continuum radiation formed at roughly the same heights as the line cores also displays a very similar CLV as the quiet Sun except for a positive offset.

Thus, changes in line blanketing also do not support the conclusion reached by (Kuhn et al. 1988). Such changes provide an important contribution to the total irradiance variations of the Sun over the solar cycle (Mitchell & Livingston 1991; Unruh et al. 1999, 2000).

Finally, sunspot umbrae show little change in contrast with μ (Albregtsen et al. 1984; Maltby et al. 1986). For such large flux tubes the hot wall effect is not expected to play a visible role and this result basically says that the temperature stratification within the umbra runs parallel to that in the quiet Sun.

3. MAGNETIC FIELDS AND THE SOLAR ENERGY FLUX

There are multiple ways in which magnetic fields can influence the energy flux passing to and through the solar surface.

a) Magnetic loops rising through the convection zone produce enhanced convection in their wake, which has been invoked by Paker (1995) as a mechanism to bring additional energy flux to the surface.

b) Magnetic flux tubes near the surface, which are nearly vertical, also block convective heat transport through them. Due to the high thermal conductivity in the convection zone the dominant part of this energy is redistributed throughout the convection zone, from where it is gradually released over a time scale of 10^5 years (e.g., Spruit 1982). Only a very small fraction of the blocked energy emerges in the surroundings of the flux tubes. This is true in particular for sunspots for which only a few percent of the blocked flux appears in a bright ring around the sunspot (Waldmeier 1939; Rast et al. 2001).

c) Due to the Wilson depression, flux tubes increase the solar surface area through which energy can escape (see Fig. 4). This excess energy also comes from the whole of the convection zone. A magnetic field at the surface can thus lead to a net brightening over the lifetime of a flux tube. A group of small flux tubes increases the total radiating surface area far more efficiently than a single sunspot (carrying the same amount of magnetic flux).

d) Waves excited within flux tubes by the convection (Roberts & Ulmschneider 1997) transport energy into the upper photosphere, chromosphere or higher layers, where it is deposited. Similarly, foot-point motions due to convection can lead the field into a stressed state of a higher energy density from which it can return to a lower energy state, e.g. through magnetic reconnection. In the process the surrounding plasma gets heated. Thus energy that would have escaped from the solar surface mainly in the visible band is transferred by magnetic processes to shorter or longer wavelengths, and into the cores of chromospheric lines such as Ca II K (Figure 1).

e) The magnetic field has an, as yet not completely understood, influence on the convection. This is seen at the solar surface in the form of abnormal granulation in magnetic regions (e.g. Title et al. 1989; Brand & Solanki 1990)

In summary, the magnetic field leads to a redistribution of the solar output in wavelength and height of emission. The surface field can also lead to a brightening or darkening of the Sun as a whole on a time scale shorter than 10^5 years.

4. THE MAGNETIC FIELD AND CYCLIC CHANGES IN SOLAR RADIANCES

At a given point on the solar surface, the brightness changes over the solar cycle. The magnetic field at the solar surface contributes in 3 ways to such changes.

1. The total amount of magnetic flux within a given surface area can change. Thus, the number of flux tubes increases from activity minimum to maximum.

2. The types of flux tubes present can change. E.g., the distribution of flux tube sizes evolves from a sharply peaked maximum at small flux tubes to a broader distribution of sizes, at least in active regions. There the ratio of surface areas covered by small flux tubes (forming faculae) to that covered by large flux tubes

(sunspots) varies by roughly a factor of 2 over the solar cycle (Chapman et al. 1997). The log-normal size distribution function of sunspots does not vary significantly over the solar cycle, however, except in amplitude (Bogdan et al. 1988). A more detailed analysis does reveal a weak trend towards larger sunspots with increasing activity (Solanki & Unruh 2002).

3. The properties of individual flux tubes can change over the solar cycle. Thus the brightness of sunspot umbrae is thought to increase by roughly 20% from the beginning to the end of a cycle (Albregtsen & Maltby 1978; Albregtsen et al. 1984) and the average penumbral to umbral area ratio also varies (Jensen et al. 1956). Both effects produce a dependence of the average sunspot contrast on the phase of the solar cycle.

An illustration of the first of the effects listed above is given by the work of Schühle et al. (2000) and Pauluhn & Solanki (2002). The former authors found that the EUV radiances measured by SUMER (Solar Ultraviolet Measurement of Emitted Radiation, Wilhelm et al. 1995) in various spectral lines from quiet Sun areas near solar disc centre have been increasing with increasing solar activity. This is surprising, since the quiet Sun is not a priori expected to change over the cycle (but see Harvey & White 1999). Pauluhn & Solanki (2002) show that the magnetic flux, in particular in stronger elements, also increased in the observed quiet Sun areas. They obtained a good correlation between the temporal evolution of the total magnetic flux and of the radiance in, e.g., He I 584Å. There is thus an intimate connection between solar cycle time scale radiance variations and the magnetic flux.

A significant portion of the magnetic flux in major active regions lies in sunspots, which partly compensate the brightening due to faculae in the active region. Therefore, large active regions do not contribute as strongly to the total brightening of the Sun as smaller active regions or the enhanced network (which is partly fed by decaying active regions). The situation is even more extreme on very active Sun-like stars. Whereas stars with an activity level similar to the Sun also become brighter with increasing magnetic activity level, highly active stars exhibit the opposite behaviour (Radick et al. 1990; Hall 2002). I.e. on these stars the darkening due to stars-spots dominates over the brightening due to faculae.

5. SOLAR MAGNETIC FIELD AND IRRADIANCE VARIATIONS

Once models of the thermal structure of the different types of magnetic regions (such as network, faculae and sunspots), or of flux tubes of different sizes have been constructed, spectra of these features need to be obtained over all relevant wavelengths, in general the UV, visible and IR. Such spectra are needed at different μ values between 0 and 1. From such spectra the contribution of, e.g., faculae to the irradiance at a given time can be determined if the distribution of these features over the solar disc at that time is known. The latter can be (imperfectly) obtained from magnetograms and white-light images. The white-light images give the sizes and positions of sunspots and pores, while the magnetograms provide information on the faculae and the network. The information is imperfect, in particular for the network. The small signals associated with the network are not always clearly separated from the noise, so that there is a tendency to underestimate the contribution from this component. The situation is particularly bad close to the solar limb, since the regularly recorded magnetograms (Kitt Peak and MDI) so far only register the longitudinal magnetic field, so that closer to the limb the mainly vertical field in faculae and the network becomes increasingly less visible.

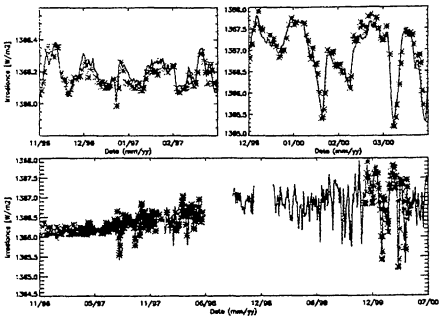

Figure 5. Reconstruction (stars) of total solar irradiance for roughly 700 individual days between the end of 1996 and mid 2000. The reconstruction covers two periods, one near the onset of solar cycle 23, the other close to its maximum. The irradiance record measured by VIRGO is represented by the solid line. The two panels on the top show a zoom-in to the beginning (left panel) and the end (right panel) of the complete dataset (lower panel), respectively. The model is able to reproduce both, short-term variations on time-scales of days to weeks as well as the longer-term increase of solar irradiance between activity minimum and maximum (from Fligge et al. 2000).

Nevertheless, using MDI (Scherrer et al. 1995) magnetograms and continuum images, as well as the spectra produced by simple plane-parallel models of the quiet Sun, faculae, sunspot umbrae and penumbrae Fligge et al. (2000) could reproduce the total irradiance variations caused by the passage of individual active regions across the solar disc, as well as the increase of irradiance from solar activity minimum to maximum. Figure 5 shows a comparison of the reconstructed irradiance with the VIRGO data. The lower frame covers a period of almost 4 years, while the upper frames show two extracts to allow a more detailed comparison. The agreement between the two time series is quite satisfactory. The agreement with both the low and the high activity values is about equally good, indicating that there is no bias in the reconstruction. Note that there is a single free parameter underlying these reconstructions that has not been constrained by independent data. It governs the conversion of the magnetogram signal strength into a facular filling factor (i.e. the area fraction covered by faculae).

At the same time the flux spectra from the employed

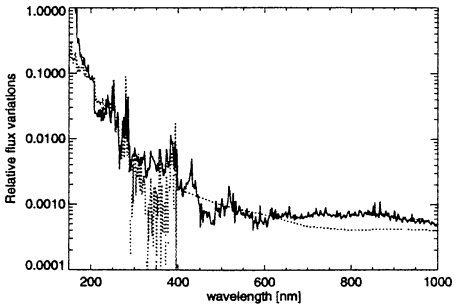

Figure 6. Relative flux (or equivalently irradiance) variations over the solar cycle vs. wavelength. The dotted curve represents observations for wavelengths shorter than 400 nm. The solid line shows the relative irradiance variations resulting from a 3-component model with a facular filling factor of 2.3% and a spot filling factor of 0.23%. The total irradiance variation predicted by the model is 0.1% (adapted from Unruh et al. 1999).

models, when combined after weighting with filling factors appropriate to sunspot maximum and minimum, reproduce the relative change in the UV flux spectrum between solar cycle maximum and minimum, as shown in Figure 6. Simply increasing the effective temperature of the Sun gives a far worse representation of the data. The model also reproduces other quantities, such as the variation over the cycle of the ratio of the surface area covered by faculae to sunspots (as measured by Chapman et al. 1997).

In spite of the simplicity of the model it manages to reproduce over 90% of the total irradiance changes over the solar cycle. Confidence in the model is increased by the fact that earlier discrepancies between the reconstructions and the VIRGO data (e.g. Solanki & Fligge 2002) were found to be due to problems in the VIRGO data. After improving the compensation for instrument degradation (Fröhlich & Finsterle 2001; cf. Lean & Fröhlich 2002) the correspondence with the model improved significantly.

In spite of the success of the model there is still considerable room for improvement. One aim is to remove the dependence on the remaining free parameter. This means constructing improved model atmospheres. A first step has been taken by Ortiz et al. (2002) and Wenzler et al. (2002). Further improvements will be to include proper flux tube physics and to extend the length of time over which the irradiance is reconstructed, including over more than one solar cycle. Longer timescales are also important for a comparison with climate.

6. MAGNETIC FIELDS AND THE SECULAR EVOLUTION OF SOLAR IRRADIANCE

There is no reliable direct evidence for the secular variation of irradiance (compare **?**, with Fröhlich & Lean 1998). Hence, as far as secular irradiance variations are concerned, the aim is not to see to what extent solar surface magnetism can explain observed irradiance variations, but rather to use the evolution of the Suns's magnetic field to deduce a possible secular evolution of the irradiance. Earlier conclusions regarding the presence of such variations over a centuries timescale were based on the different levels of Ca II H and K core emission observed on late-type field stars (Baliunas & Jastrow 1990). Since stars with lower Ca II H and K emission than the Sun at activity minimum are often in a non-cycling state, the Ca II H and K level was converted into differences in solar irradiance between the Maunder minimum and the current cyclic state of the Sun by employing the correlation between solar irradiance and Ca II H and K emission over a solar cycle (White et al. 1992; Lean et al. 1992, 1995).

Now, the Ca II H and K core emission is closely coupled with the magnetic field, so that if the former really does vary secularly then so must the latter. Unfortunately, the stellar evidence is very indirect, with numerous relatively strong assumptions underlying it. Therefore the discovery by Lockwood et al. (1999), based on historical records of geomagnetic disturbances caused by the Sun's magnetic field, that the Sun's interplanetary magnetic flux doubled in the course of a century is of considerable importance (cf. Lockwood 2002). The Sun's interplanetary magnetic flux reconstructed by Lockwood et al. (1999) is given by the green curve in Figure 7. Also plotted is the ^{10}Be concentration in Greenland ice cores (Beer et al. 1990; dotted curve). Since ^{10}Be is produced by cosmic rays, whose flux is modulated by the heliospheric field, the good correspondence between the two strengthens the conclusion of Lockwood et al. (1999). Note that the interplanetary field is the part of the heliospheric flux close to the ecliptic. The heliospheric flux is in turn identical to the Sun's open magnetic flux, which is at least to a considerable part rooted in coronal holes, i.e. in large-scale regions of predominately a single polarity (e.g. Wang 2002). This flux is known to live for multiple years on the solar surface (Wang et al. 2000). Hence open flux from a given cycle is still present on the solar surface when fresh open flux from the next cycle appears. There is thus considerable overlap between the two cycles as far as their open flux is concerned.

This implies that the Sun's open flux does not drop to zero at solar activity minimum, but forms a background whose strength depends on both the strength and the length of the preceding solar cycle. On the basis of this simple idea Solanki et al. (2002) modelled the open flux since the Maunder minimum. In Figure 7 the output of their model is plotted red. The good agreement with the other two curves again strengthens the case for a secular evolution of the Sun's open flux.

Now, the open flux only contributes a few percent to the Sun's total flux and is, on its own, not expected to provide a significant contribution to secular irradiance changes. However, the overlap between consecutive solar activity cycles is not restricted to the open flux. Harvey (1992, 1994) has shown that significant flux already starts emerging in ephemeral active regions belonging to the new cycle, while the old cycle is still in full swing. This overlap again leads to the build up of a significant background field, which is visible on the surface as quiet

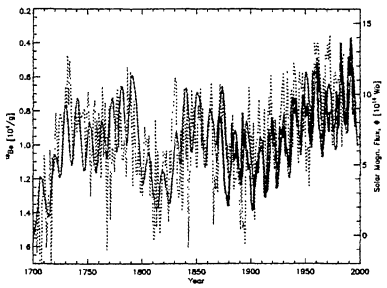

Figure 7. Evolution of the open magnetic flux at the solar surface since the end of the Maunder minimum in 1700. The flux of the interplanetary magnetic field reconstructed by Lockwood et al. (1999) from geomagnetic variations is given by the green curve, the ^{10}Be concentration in ice cores measured by Beer et al. (1990) is represented by the dotted curve (corresponding to the inverted scale on the left y-axis) and the predictions of the model of Solanki at al. (2000) are given by the red curve. The interplanetary flux values have been multiplied by a factor of 2 in order to obtain the total unsigned flux. The ^{10}Be record has been plotted without any smoothing or filtering.

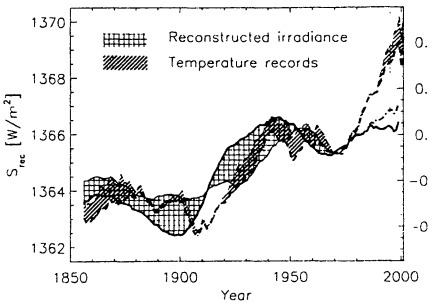

Figure 8. Total solar irradiance and terrestrial temperature vs. time. The solid curves enclosing the lightly hatched area prior to 1979 represent irradiance reconstructions (one being cycle-length based, the other cycle-amplitude based). From 1979 onwards they represent total irradiance measurements (solid: composite of Fröhlich and Lean 1998; dot-dashed: composite following Willson 1997). The dashed curves enclosing the heavily hatched region represent northern hemisphere and global temperatures. All curves have been smoothed by an 11-year running mean. After the epoch marked by the vertical dotted line the averaging period has been successively reduced.

network. This background is always present when the Sun is in a cyclic state, but can show secular variations depending on the strength and length of the solar cycle.

Thus, it is expected that the total magnetic flux exhibits a secular variation similar to that displayed by the open flux in Figure 7. This has been confirmed by Solanki et al. (2002), who compute the evolution of the magnetic flux emerging in active regions and ephemeral active regions separately. Since little flux was emerging during the Maunder minimum to replenish decaying (cancelling) flux, it is expected that near its end, around 1700, little magnetic flux was present on the solar surface. Since then a significant amount of background flux has been built up. There is more background flux than suggested by Kitt Peak synoptic charts (Harvey 1994) and may be over double that amount (Krivova et al. 2002). The functional form of the secular variation of the total background magnetic flux is very close to that displayed in Figure 7.

Since the background flux is composed almost entirely of small and bright flux tubes, such as form the magnetic network, a variation in this flux will cause directly proportional variations in irradiance. From Figure 7 we expect solar total irradiance also to have increased since 1700.

In Figure 8 one sees solar irradiance since roughly 1850 together with global and northern hemisphere temperatures. Up to 1980 the plotted irradiance curves result from two different reconstructions (which differ mainly in the assumptions underlying the secular trend; Solanki & Fligge 1999). They have been scaled such as to best match the temperature records prior to 1975 (Krivova & Solanki 2002).

It is evident from Figure 8 that although the irradiance correlates rather well with climate (and leads climate changes by 0-10 years) over most of the time covered by the figure, the two diverge significantly during the last quarter of a century. Thus, even if solar irradiance variations accounted for most of climate change prior to 1975, from Figure 8 it is clear that they have not significantly contributed to the very steep and strong global warming. This conclusion is supported by recent climate modelling (see Lockwood 2002).

REFERENCES

Albregtsen F., Maltby P., 1978, *Nature* 274, 41

Albregtsen F., Joràs P.B., Maltby P., 1984, *Solar Phys.* 90, 17

Baliunas S.L., Jastrow, 1990, *Nature* 348, 520

Beer J., Blinov A., Bonani G., et al., 1990, *Nature* 347, 164

Bogdan T.J., Gilman P.A., Lerche I., Howard R., 1988, *Astrophys. J.* 327, 451

Brand P.N., Solanki S.K., 1990, *Astron. Astrophys.*, 231, 221

Briand C., Solanki S.K., 1995, *Astron. Astrophys.*, 299, 596

Chapman G.A., Cookson A.M., Dobias J.J., 1997, *Astrophys. J.* 482, 541

Fligge M., Solanki S.K., Meunier N., Unruh Y.C., 2000, in: *Proc. 1st Solar & Space Weather Euroconference "The Solar Cycle and Terrestrial Climate"*, A. Wilson (Ed.), ESA SP-463, Noordwijk, 117

Foukal P.,, Fowler L., 1984, *Astrophys. J.*, 281, 442

Foukal P., Harvey K., Hill F., 1991, *Astrophys. J.*, 383, L89

Frazier E.N., 1971, *Solar Phys.*, 21, 42

Fröhlich C., Lean J., 1998, *Geophys. Res. Lett.*, 25, 4377

Fröhlich C., Finsterle W., 2001, in: *Recent Insights into the Physics of the Sun and Heliosphere: Highlights from SOHO and Other Space Missions*, P. Brekke, B. Fleck, J.B. Gurman (Eds.), *Astron. Soc. Pacific IAU Symp.*, 105

Grossmann-Doerth U., Knölker, M., Schüssler M., Solanki S.K., 1994, *Astron. Astrophys.*, 285, 648

Hall J., 2002, there proceedings

Harvey K.L., 1992, in: *The Solar Cycle*, K.L. Harvey (Ed.), *ASP Conf. Ser.*, Vol. 27, p. 335

Harvey K.L., 1994, in: *Solar Surface Magnetism*, R. J. Rutten, C.J. Schrijver (Eds.), Kluwer, Dordrecht, p. 347

Harvey K.L., White O.R., 1999, *Astrophys. J.*, 515, 812

Jensen E., Nordø J., Ringnes T.S., 1956, *Ann d'Astrophys.*, 19, 165

Keller C.U., 1992, *Nature*, 359, 307

Knölker M., Schüssler M., 1988, *Astron. Astrophys.*, 202, 275

Krivova N., Solanki S.K., 2002, *J. Geophys. Res.* submitted

Krivova N., Solanki S.K., Fligge M., 2002, these proceedings

Kuhn J.R., Libbrecht K.G., Dicke R.H., 1988, *Science*, 242, 908

Lean J., Skumanich A., White O., 1992, *Geophys. Res. Lett.*, 19, 1595

Lean J., Beer J., Bradley R., 1995, *Geophys. Res. Lett.*, 22, 3195

Lean J., Fröhlich C., 2002, these proceedings

Leighton R.B., 1959, *Astrophys. J.* 130, 366

Lockwood M., Stamper R., Wild M.N., 1999, *Nature*, 399, 437

Lockwood M., 2002, these proceedings

Maltby P., Avrett E.H., Carlsson M., Kjeldseth-Moe O., Kurucz R.L., Loeser R., 1986, *Astrophys. J.*, 306, 284

Mitchell W.E., Jr., Livingston W.C., 1991, *Astrophys. J.*, 372, 336

Ortiz A., Solanki S.K., Domingo V., Fligge M., Sanahuja B., 2002, *Astron. Astrophys.*, submitted

Parker E.N., 1995, *Astrophys. J.*, 440, 415

Pauluhn A., Solanki S.K., 2002, these proceedings

Radick R.R., Lockwood G.W., Baliunar S.L., 1990, *Science* 247, 39

Rast M.P., Meisner R.W., Lites B.W., Fox P.A., White O.R., 2002, *Astrophys. J.*, 557, 864

Roberts B., Ulmschneider P., 1997, in: *Solar and Heliospheric Plasma Physics*, C.E. Alissandrakis, G. Simnett, L. Vlahos (Eds.), *Proc. 8th European Meeting on Solar Physics*, Springer, Berlin, p. 75

Scherrer P.H., BogartR.S., Bush R.I., Hoeksema J.T., Kosovichev A.G., Schou J., Rosenberg W., Springer L., Tarbell T.D., Title A., Wolfson C.J., Zayer I. and the MDI Engineering Team, 1995, *Solar Phys.*, 162, 129

Schrijver C.J., Coté J., Zwaan C., Saar S.H., 1989, *Astrophys. J.*, 337, 964

Schühle, U., Wilhelm, K., Hollandt, J., Lemaire, P., Pauluhn, A., 2000, *Astron. Astrophys.*, 354, L71

Skumanich A., Smythe C., Frazier E.N., 1975, *Astrophys. J.*, 200, 747

Skumanich A., Lean J.L., Livingston W.C., White O.R., 1984, *Astrophys. J.*, 282, 776

Solanki S.K., Brigljević V., 1992, *Astron. Astrophys.*, 262, L29

Solanki S.K., Fligge M., 1999, *Geophys. Res. Lett.*, 26, 2465

Solanki S.K., Schüssler M., Fligge M., 2000, *Nature*, 408, 445

Solanki S.K., Schüssler M., Fligge M., 2002, *Astron. Astrophys.*, 383, 706

Solanki S.K., Fligge M., 2002, *Adv. Space Res.*, in press

Solanki S.K., Unruh Y.C., 2002, *Monthly Notices Royal Astron. Soc.*, submitted

Spruit H.C., 1976, *Sol. Phys.*, 50, 269

Spruit H.C., 1982, *Astron. Astrophys.*, 108, 56

Sütterlin P., 1998, *Astron. Astrophys.*, 333, 305

Title A.M., Tarbell T.D., Topka K.P., Ferguson S.H., Shine R.A., et al., 1989 *Astrophys. J.*, 336, 475

Topka K.P., Tarbell T.D., Title A.M., 1992, *Astrophys. J.*, 396, 351

Topka K.P., Tarbell T.D., Title A.M., 1997, *Astrophys. J.*, 484, 479

Unruh Y.C., Solanki S.K., Fligge M., 1999, *Astron. Astrophys.*, 345, 635

Unruh Y.C., Solanki S.K., Fligge M., 2000, *Space Sci. Rev.*, 94, 145

Waldmeier M., 1939, *Astron. Mitt. Zürich* No. 138, p. 439

Wang Y.-N., 2002, these proceedings

Wang Y.-N., Sheeley N.R., Lean J., 2000, *Geophys. Res. Lett.*, 27, 621

Wenzler T., Solanki S.K., Fluri D., Frutiger C., Fligge M., Ortiz A., 2002, these proceedings

White O.R., Skumanich A., Lean J., Livingston W.C., Keil S.L., 1992, *Publ. Astron. Soc.*, 104, 1139

Wilhelm K., Curdt W., Marsch E., Schühle U., Lemaire P., Gabriel A.H., Vial J.-C., Grewing M., Huber M.C.E., Jordan S.D., Poland A.I., Thomas R.J., Kühne M., Timothy J.G., Hassler D.M., Siegmund O.H.W., 1995, *Solar Phys.*, 162, 189

Willson R.C., 1997, *Science*, 277, 1963

Woods T., 2002, these proceedings

Zwaan C., Cramer L.E., 1989, in: *FGK Stars and T Tauri Stars*, L.E. Cram, L.V. Kuhi (Eds.), NASA SP-502, Washington, p. 215